

CHAPTER - 1

Introduction

1.1 Nuclear Physics far from the stability	03
1.2 Heavy ion reactions	04
1.2.1 Elastic scattering	07
1.2.2 Inelastic scattering	07
1.2.3 Transfer reactions	08
1.2.4 Quasielastic scattering	08
1.2.5 Deep inelastic scattering	08
1.3 Coulomb barrier	08
1.4 General Motivation of the thesis	11
1.4.1 Fusion and Breakup of weakly bound nuclei	11
1.4.2 Elastic scattering in collisions of weakly bound nuclei	14
1.5 Brief literature survey	25
1.6 Plan of the thesis	26
References	29

In the last few decades a great deal of attention has been drawn towards the study of fusion of two many-body systems, such as the atomic nucleus or atomic clusters, can be described, to a great degree of precision, by a model involving just the radial distance between the centers of mass of the two objects. The fundamental quantum mechanical tunneling phenomenon is purported to operate in a full-fledged fashion allowing a quantitative description of the “fusion” of the two nuclei. Reference to the many-body nature of the system is made through significant, albeit simple, deviation from the Barrier Penetration Model (BPM). The fusion of nuclei, an important phenomenon of paramount importance in the artificial, laboratory, generation of energy and in the stellar interior through nucleosynthesis, as well as in the quest for superheavy elements with charges and masses significantly larger than the actinide nuclei, has received a great amount of attention over the last four or so decades, owing to the availability of heavy-ion accelerators.

During the 1960s and 1970s most of the attention was directed towards the study of nuclear fusion at center of mass energies higher than the natural threshold for processes induced by the short-range strong hadronic force, the so-called Coulomb barrier. Several experiments for fusion measurements of easily breakable stable nuclei such as ${}^6\text{Li}$, ${}^7\text{Li}$ and ${}^9\text{Be}$ with heavy targets were reported and the reduction in the fusion cross section was confirmed. The status of the fusion of weakly bound stable and unstable nuclei is therefore that of an ongoing extensive effort both in theory and experiment.

It is important to study the elastic scattering on different projectile target combinations with varying asymmetry, in order to understand more complicated reactions. The cross-section of elastic scattering can help to obtain an optical potential which is necessary to understand the entrance and exit channel potentials of some transfer reactions. Breakup effects also play an important role in the scattering mechanism, affecting the interaction potential. One of the important points of investigation is whether the effect of breakup is essential to increase the total reaction cross-section. Therefore, it is important to investigate the dependence of the breakup and total reaction cross-sections near the barrier energies.

1.1 Nuclear Physics far from the stability

The enormous work done on nuclear physics in the 1950s, 60s and 70s was mainly focused on nuclei close to stability, due to the limited ability to produce unstable nuclei. Thus the knowledge on nuclear physics extracted in that period was mostly based on the about 300 stable nuclei (compare to the about 6000 nuclei that has been predicted by theory to be particle bound). This knowledge was in the 80s found to be incomplete when it became possible to study unstable nuclei at facilities such as ISOLDE at CERN, RIKEN in Japan, MSU in USA, GANIL in France and several other places. One of the first discoveries that changed the traditional view of nuclear physics was that of a neutron halo structure observed by Tanihata *et al* in ${}^6,8\text{He}$ [1] and ${}^{11}\text{Li}$ [2].

To explore nuclei further and further away from stability is not an easy task and demands an ongoing development of production and detection techniques. The evolution of the nuclear chart is shown in Fig. 1.1 where the development from about 800 isotopes in the 40s to about 3000 isotopes today is visualized. Within the last 20 years about 1/3 of all known isotopes has been discovered and hence the basis for extending nuclear theories to unstable nuclei has been greatly improved.

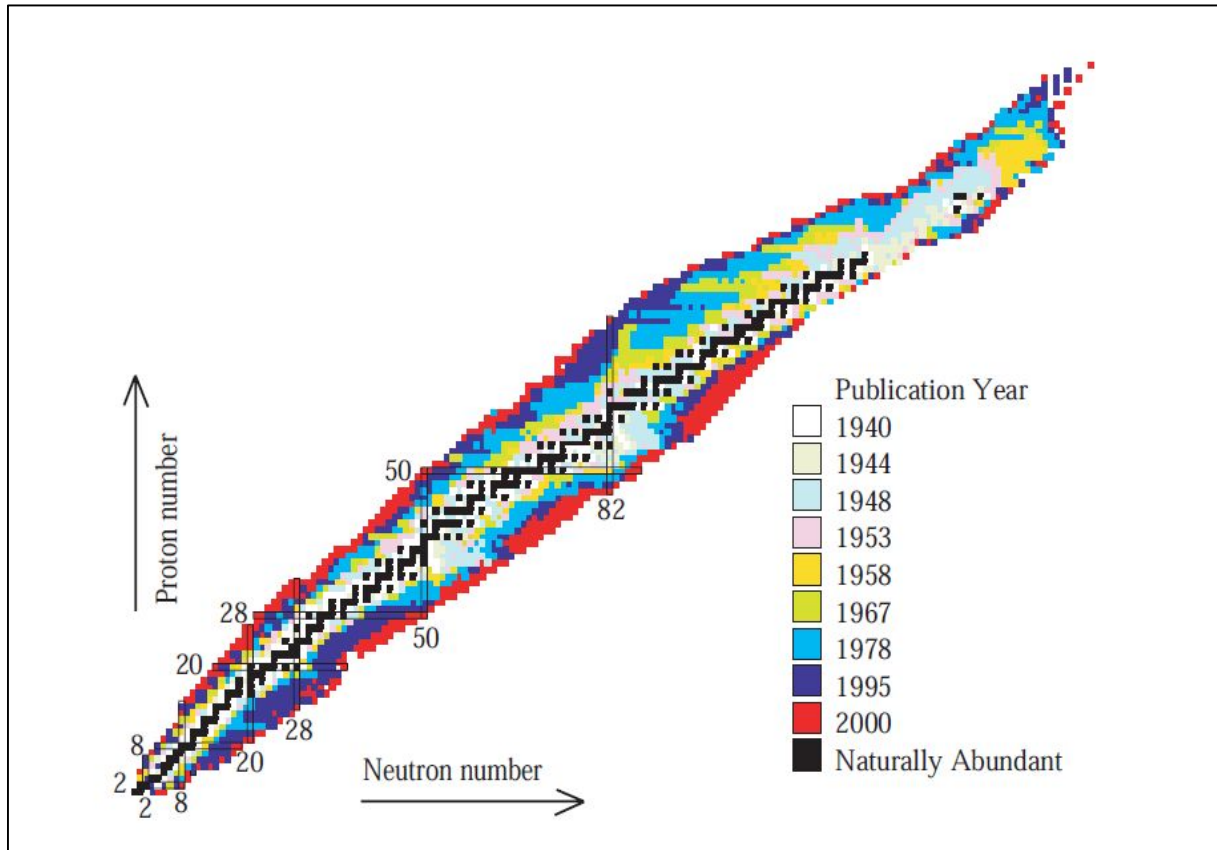
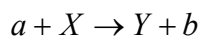


Figure 1.1 Historic nuclear chart with color indications of year of discovery. Note that many nuclei discovered since 1978.

1.2 Heavy ion reactions

A nuclear reaction is a process whereby a nucleus is transformed from one species to another. These reactions involve the collision of an accelerated projectile with a target nucleus. In these reactions the initial system is transformed into the final system, consisting of the products of the reaction. Symbolically a nuclear reaction is represented as, [3];



where a is the accelerated projectile, X is the target (usually stationary in the laboratory), Y and b are the reaction products. Usually, Y is the heavy product and b are light particles that can be detected e.g. α -particles, γ -rays, neutrons etc. [4]. According to the classical picture, the

projectile can induce various kinds of reactions depending on the impact parameter or the corresponding angular momentum.

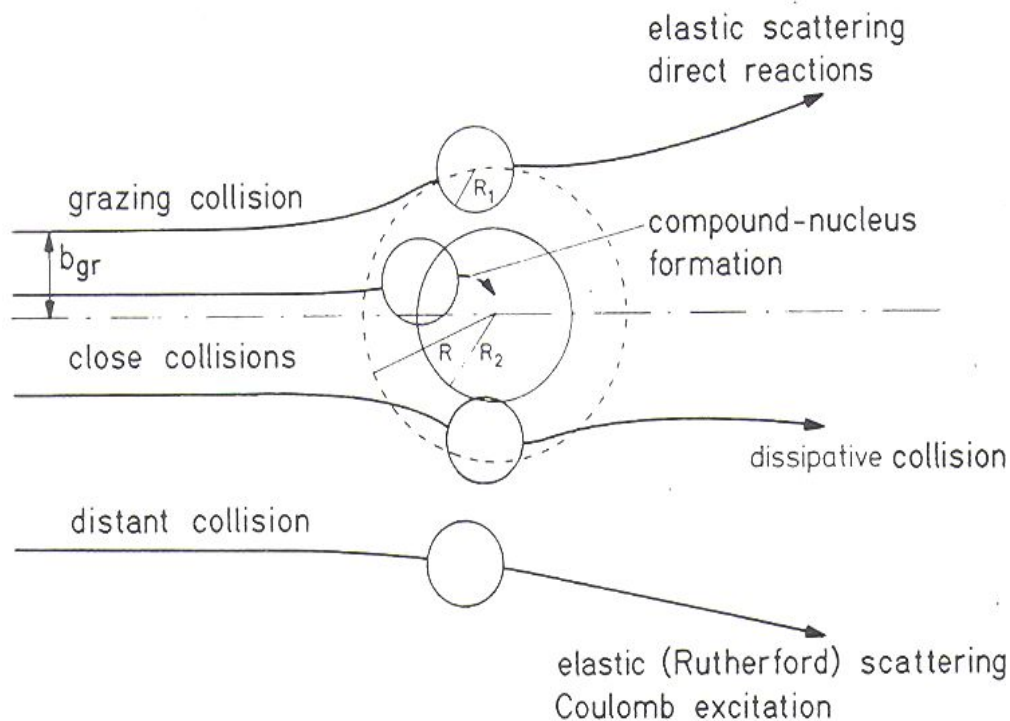


Figure 1.2 Distant, grazing and close collisions in the classical picture of heavy ion collisions, from [5].

For heavy systems the various reaction channels can be referred to as elastic scattering, inelastic scattering, transfer reactions, fusion reactions, fission reactions and quasi-fission reactions. Fig. 1.2 and Fig. 1.3 illustrate the various nuclear reactions. The parameters used in these figures are b_{gr} an impact parameter for a grazing collision, R_t a target radius, R_p a projectile radius and r_{int} an interaction radius.

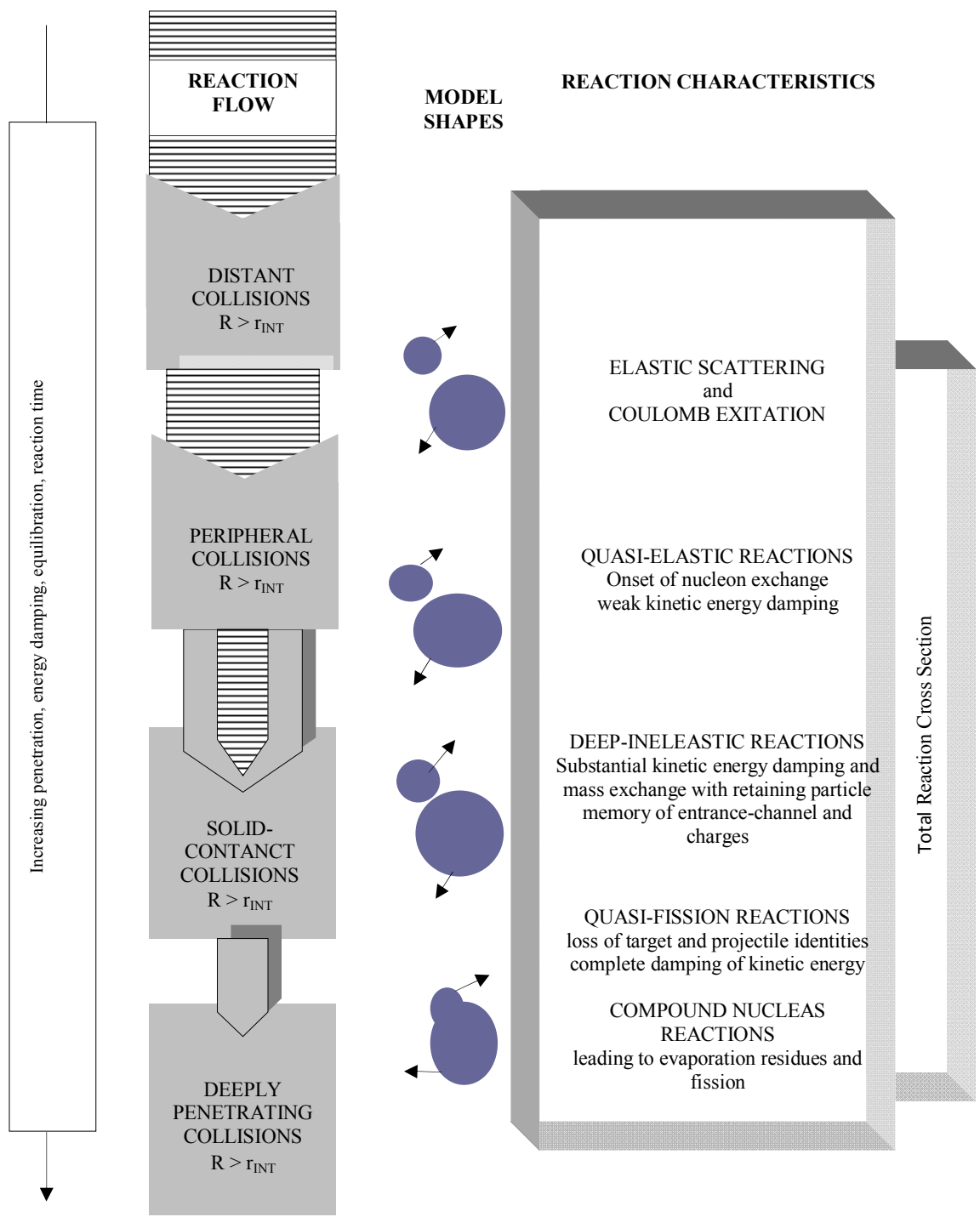
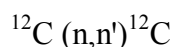


Figure 1.3 Schematic classification of heavy-ion reactions, from [6].

1.2.1 Elastic Scattering

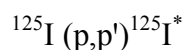
In nuclear reaction $A(a,b)B$, a and A are projectile and target, respectively and b and B are the outgoing ejectile and product nucleus respectively. If the outgoing particle i.e., ejectile is identical to the incident particle, the reaction is called scattering. If the energy of the target nucleus is left unchanged in the process, it is called elastic scattering. An example of elastic scattering is given below:



In this example, a neutron in the vicinity of ^{12}C nucleus gets scattered, i.e. its direction is changed and kinetic energy is reduced. It means that ^{12}C nucleus is set into motion by the neutron at the expense of its own kinetic energy. The outgoing particle is, therefore, the original neutron with lower kinetic energy. Kinetic energy of the projectile is changed but total kinetic energy is conserved and potential energy is not changed. This is one of the most probable reactions that take place in moderation of neutrons in a nuclear reactor. Elastic scattering is possible with all energies of projectile.

1.2.2 Inelastic Scattering

In a scattering process if the target nucleus is left in an excited state, it is called inelastic scattering. Inelastic scattering is a similar reaction, where the projectile and ejectile are same but both kinetic energy and potential energy are changed, and the total energy is conserved. An example of elastic scattering is given below:



Here also the kinetic energy of the projectile is reduced and the target nucleus ^{125}I is excited to a higher energy and thus its potential energy changed. Inelastic scattering needs a minimum energy corresponding to the first excited state in the target nucleus. Excited nucleus deexcites by gamma decay.

1.2.3 Transfer reactions

In transfer reactions, when the projectile passes over the periphery of the target one or more nucleons are transferred between the projectile and the target, such as an incoming deuteron turning into an outgoing proton or neutron, thereby adding some nucleons to the target A to form a nucleus, B.

1.2.4 Quasielastic scattering

In quasielastic scattering the projectile loses a moderate amount of energy and exchanges a few nucleons with the target nucleus. Quasielastic reactions are assumed to correspond to collisions in which the surfaces of the two ions have just been in a grazing contact. However, in this study, quasielastic scattering will refer to the sum of all the elastic scattering, inelastic scattering and transfer reactions.

1.2.5 Deep inelastic scattering

This reaction entails substantial damping of kinetic energy and mass exchange. The larger fragments are highly deformed and excited while retaining partial memory of “target” and “projectile” masses and charges [7]. This process takes place at energies above the Coulomb barrier.

1.3 The Coulomb barrier

Due to the electrostatic repulsion present between the positively charged target nucleus and the positively charged projectile there is difficulty in the penetration of the much familiar barrier known as the Coulomb barrier. The system is straightforwardly described in terms of their relative motion in the center-of-mass system, as the two associates are of comparable mass. Assuming the standard laboratory situation of a fixed target, which is bombarded with a beam of projectile nuclei, the relation between the kinetic energy E_{lab} as measured in the laboratory system and the kinetic energy E_{cm} in the center-of-mass system is given by

$$E_{cm} = \frac{A_t}{A_t + A_p} E_{lab} \quad (1.1)$$

where A_p and A_t represent the mass number of the projectile and target nuclei, respectively. Electron mass and differences in binding energy per nucleon may be ignored as a good approximation. The motion of the center-of-mass is fully determined by the kinematics of the reaction and can be calculated from the bombarding energy and the nuclear masses. Quantum mechanically the nuclear binary system may be represented by the wave function $\Psi(r)$. Using the center-of-mass parameterization, the combined effect of the Coulomb and the nuclear force between the two nuclei can be expressed as the interaction potential. These have been illustrated in Fig. 1.4.

$$V(r) = V_C(r) + V_n(r) \quad (1.2)$$

where V_C are the Coulomb and V_n the nuclear potential. The motion of the binary system is then described by the Schrödinger equation.

$$\left[-\frac{\hbar^2 d^2}{2\mu dr^2} + \frac{l(l+1)\hbar^2}{2\mu r^2} + V(r) - E \right] \Psi(r) = 0 \quad (1.3)$$

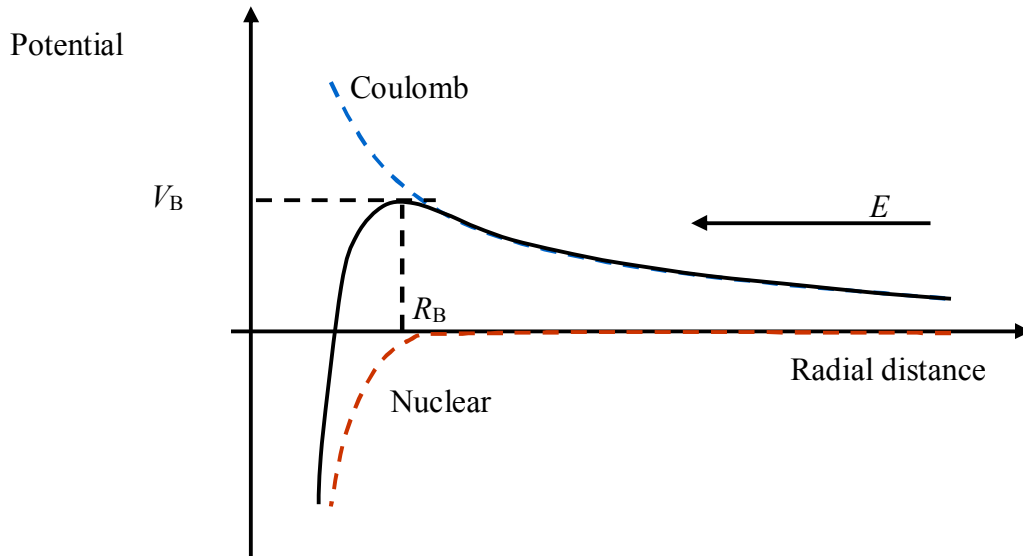


Figure 1.4 The illustration of the forces that form a Coulomb barrier between the participating nuclei in a nuclear reaction.

At large distances r , the Coulomb potential V_C has the form of the electrostatic potential for two point-charges. At close approach, when the charge distributions overlap, the point-charge has to be modified. This is often achieved by replacing one of the point charges with a homogeneously charged sphere of radius R_C , so that

$$V_C(r) = Z_p Z_t e^2 \begin{cases} 1/r & \text{for } r > R_C \\ \left(\frac{2}{3} - \frac{r^2}{2R_C^2} \right) / R_C & \text{for } r \leq R_C \end{cases} \quad (1.4)$$

Since during the collision there occur a large number of interactions between the projectile and the target nucleons, it has not been possible to determine the nuclear potential V_n from the known two-body forces between nucleons. It is therefore common practice to make a simple parameterization, approximating the nuclear potential with a function which resembles the nuclear mass distribution. This results in the Woods-Saxon potential

$$V_n(r) = \frac{-V_0}{1 + \exp(r - R_n/a_0)} \quad (1.5)$$

where V_0 refers to the potential depth and a_0 is the diffuseness of the potential. The radius R_n of the nuclear potential is given by;

$$R_n = r_0 \left(A_p^{\frac{1}{3}} + A_t^{\frac{1}{3}} \right) \quad (1.6)$$

where r_0 is the radius parameter. It is worthwhile to mention that the potential parameters V_0 , a_0 and r_0 are not unique. Hence they are usually adjusted by fitting experimental data.

1.4 General Motivation of the thesis

The main motivation of the present thesis is to understand the reaction mechanism involving weakly bound nuclei (${}^6\text{Li}$ & ${}^7\text{Li}$) and radioactive ion beam (${}^8\text{Li}$), where the prime focus is on the study of elastic scattering and the breakup of such projectiles. The prime objective of the present thesis is to understand reaction mechanism using the weakly bound systems and radioactive ion beams. Precise elastic scattering angular distributions were measured, at near barrier energies, for the weakly bound systems viz., ${}^6,7\text{Li} + {}^{116}\text{Sn}$ and ${}^6\text{Li} + {}^{112}\text{Sn}$ and two different energies for radioactive ion beams viz., ${}^8\text{Li} + {}^9\text{Be}$, ${}^{51}\text{V}$. The nuclei used in the present thesis, have very low breakup threshold energies and so they have a large breakup (BU) probability. The significance and challenges in studying such nuclei are presented here.

1.4.1 Fusion and breakup of weakly bound nuclei

The fusion of weakly bound nuclei differs in a fundamental way from that of tightly bound ones in so far as the influence of the breakup channel is concerned [8]. Whereas this channel does play an important role in reducing the fusion cross section of the latter well above the Coulomb barrier, the effect in the former is felt in the vicinity of the Coulomb barrier, owing to the small Q -value involved. What accompanies breakup is the occurrence of Incomplete Fusion (ICF) whereby part of the mass of the broken projectile is captured by the target, while

one or more fragments fly away from the interaction region. Such process competes with the Complete Fusion (CF), where the whole projectile is absorbed by the target. From the experimental point of view, distinguishing these two processes is a very difficult task, which can only be carried out for some particular projectile–target combinations. For this reason, operational definitions of CF and ICF are usually adopted. CF is defined as the process in which the total projectile charge fuses with the target while ICF occurs when some charged fragment survives the fusion process. In fact, other processes also contribute, as shown in Fig. 1.5. The different contributions are depicted in a varying degree of complexity. The direct complete fusion (DCF) involves the capture of the whole projectile by the target without explicitly going through the breakup channel. The sequential complete fusion (SCF) is the process when breakup does occur followed by the successive capture of the two fragments. The CF cross section is the sum

$$\sigma_{\text{CF}} = \sigma_{\text{DCF}} + \sigma_{\text{SCF}} \quad (1.7)$$

ICF corresponds to the process where one charged fragment is captured by the target while the remaining nucleons of the projectile escape from the interaction region. If both fragments represented in Fig. 1.5 are charged, the ICF cross section is given by the sum

$$\sigma_{\text{ICF}} = \sigma_{\text{ICF1}} + \sigma_{\text{ICF2}} \quad (1.8)$$

Finally, the process where breakup occurs but none of the fragments is captured is designated by elastic breakup (EBU). The corresponding cross section would contain all possible target excitations. We should emphasize that if the captured fragment is neutral, the corresponding process would be only a mass transfer, such as seen in the ${}^6\text{He} + {}^{238}\text{U}$ system [9], where the two neutrons in the halo are transferred to the target.

The difficulty in measuring CF and ICF renders the study of the fusion of weakly bound nuclei quite challenging. Further, this difficulty is shared by theory as well. In order to account for both CF and ICF one needs to develop a three-body reaction theory with absorption. Not having such a theory currently available one resorts to approximate schemes. The breakup

channel is described by the CDCC method. The continuum that describes the breakup channel is discretized into bins [10,11]. Since the resulting many coupled-channels still represent a binary system [12], this method cannot evaluate the contribution from the sequential process to the CF cross section and their estimates of the ICF cross sections may be inaccurate. Other approaches rely on the use of formulae developed for inclusive breakup to calculate the ICF cross section [13,14]. Extending such description to the calculation of CF requires the introduction of genuine three-body optical potential [15], a rather alien concept to conventional reaction theory.

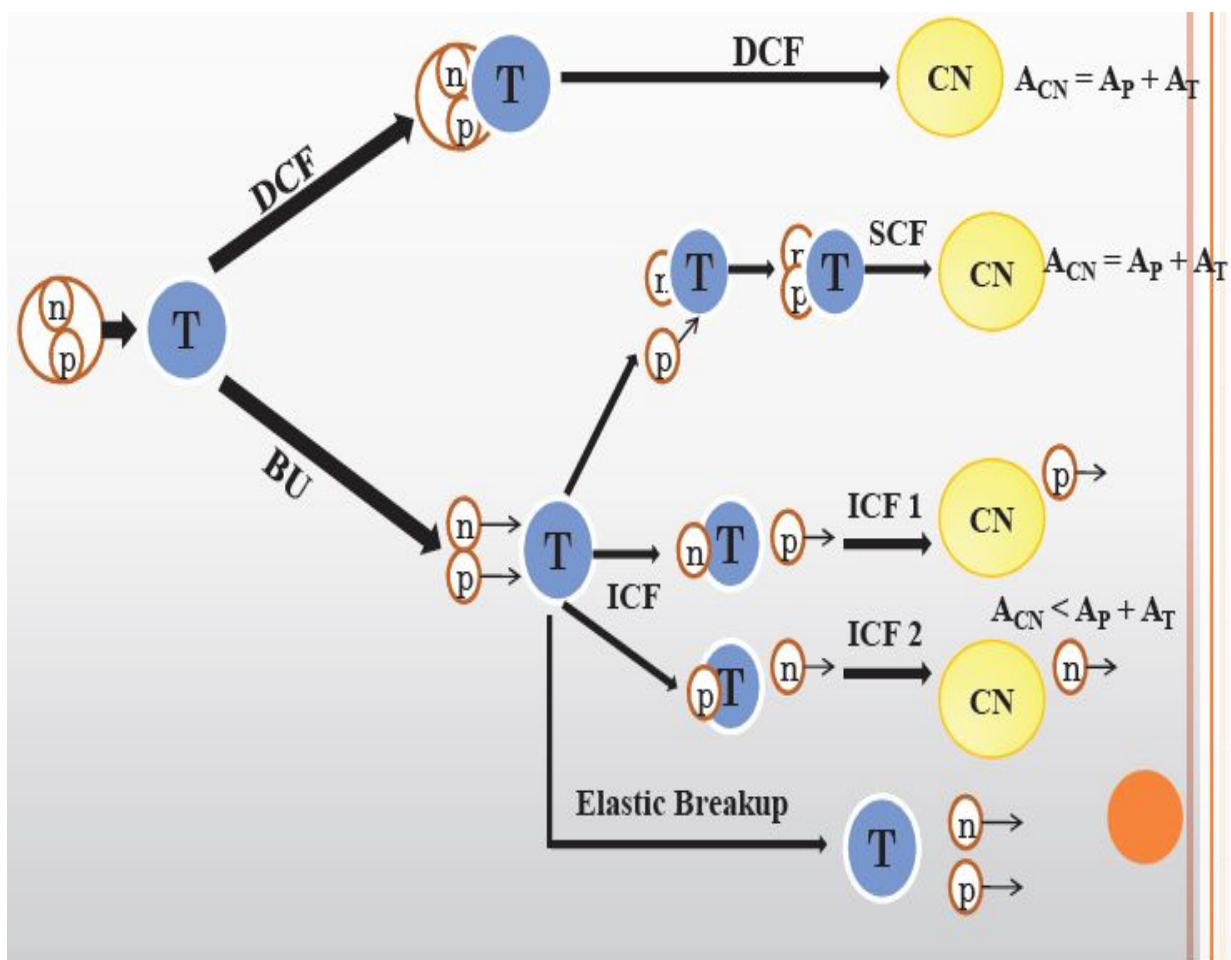


Figure 1.5 Schematic representations of the fusion and breakup processes that can take place in the collision of a weakly bound projectile. For the sake of simplicity it is assumed that the breakup produces two fragments.

1.4.2 Elastic scattering in collisions of weakly bound nuclei

An alternative method to study the influence of the breakup process on the fusion cross section of systems with weakly bound nuclei is through the elastic scattering analysis. The behavior of the energy dependences of the real and imaginary parts of the potential, at energies close to the Coulomb barrier and at the strong absorption radius, is related with the couplings between reaction channels at this energy region. In the scattering of tightly bound projectiles, the usually observed phenomenon is known as the threshold anomaly [16 – 18].

In 1994, Keeley et al. [19] studied the elastic scattering of ${}^6,7\text{Li}$ by ${}^{208}\text{Pb}$ and briefly mentioned in [8]. Very accurate and complete angular distributions were obtained for several energies, ranging from the Coulomb barrier to more than twice this value. For this purpose, they used an array of three position sensitive silicon surface barrier detector telescopes. An optical model analysis of the data was performed with a double-folding real potential and an imaginary part parameterized as a Woods–Saxon function. The real and imaginary potentials were evaluated at a small separation, close to the strong absorption radius. The results for ${}^7\text{Li}$ and ${}^6\text{Li}$ are shown on the left and on the right panels of Fig. 1.6, respectively. As can be seen, there are striking differences between the potentials for the two isotopes, both in the real and in the imaginary parts. The real potential for ${}^7\text{Li}$ shows the usual bell shape as a function of energy, while the strength of the imaginary part decreases as the bombarding energy decreases towards the barrier height. The results for ${}^6\text{Li}$ are very different and the usual threshold anomaly is not observed. The strength of the imaginary potential at the surface is much higher than in the case of ${}^7\text{Li}$, and it increases as the energy decreases.

On the other hand, the opposite happens with the real potential, which decreases near the barrier energy. A possible explanation for such behavior [19] was attributed to the presence of a repulsive polarization potential arising mainly from the effects of breakup coupling to the continuum. It was suggested that the Coulomb breakup of ${}^6\text{Li}$ on the field of the ${}^{208}\text{Pb}$ target should be important even below the Coulomb barrier. The different behaviors of the two Li isotopes was supposed to arise from the fact that ${}^7\text{Li}$ has one bound excited state strongly coupled to the entrance channel whereas ${}^6\text{Li}$ has a lower breakup threshold and no bound excited state. At energies around the barrier, the reaction cross section for the ${}^6\text{Li} + {}^{208}\text{Pb}$ system is larger than that for ${}^7\text{Li} + {}^{208}\text{Pb}$. This is mainly due to the larger breakup cross section for the former

system. Keeley and Rusek [20] performed CC calculations for the ${}^7\text{Li} + {}^{208}\text{Pb}$ system and concluded that the one neutron stripping channel produces polarization potentials with the same energy dependence as the one obtained from the data. CDCC calculations performed by the same authors [21] confirm the behaviors for the two Li isotopes obtained from the data. Keeley et al. [22] performed CDCC calculations for the ${}^7\text{Be} + {}^{208}\text{Pb}$ system, in order to test whether the scattering of ${}^7\text{Be}$, which is the ${}^7\text{Li}$ mirror nucleus but has threshold breakup energy similar to ${}^6\text{Li}$, behaves like ${}^7\text{Li}$ or ${}^6\text{Li}$. The calculations show that the behavior of the ${}^7\text{Be}$ scattering is similar to that of ${}^6\text{Li}$, which means that the breakup threshold is the controlling factor in determining the near barrier behavior of the dynamic polarization potential. However, elastic scattering experiments with polarized ${}^7\text{Li}$ beams on ${}^{208}\text{Pb}$ [23,24] have not shown conclusive results. Although the authors interpreted their results as if there is the usual threshold anomaly for this system, a careful observation of Fig. 1.7 may lead to controversial interpretations, since the transition terms of the nuclear optical potential at the strong absorption radius do not have the usual behavior. Actually, the transitional imaginary potential increases as the energy decreases towards the barrier.

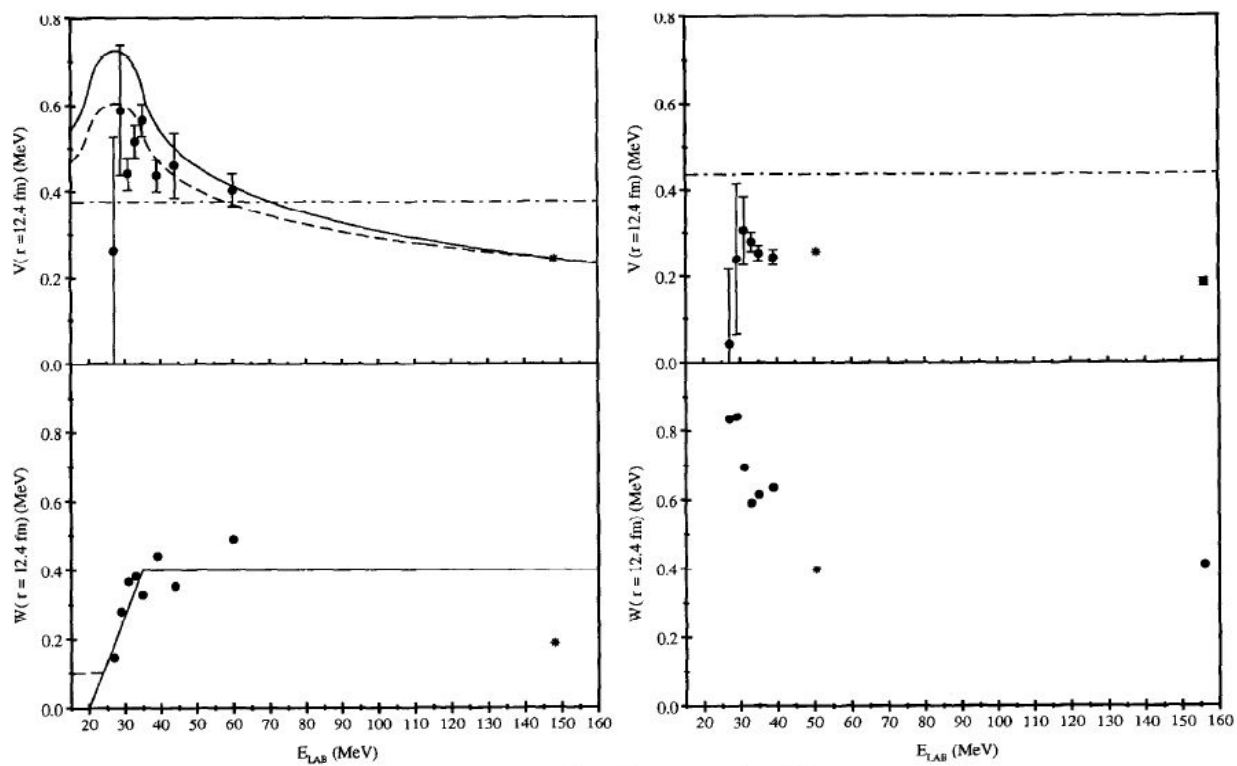


Figure 1.6 Best-fit real and imaginary potentials, at the strong absorption radius, for the elastic scattering of ${}^7\text{Li} + {}^{208}\text{Pb}$ (left) and ${}^6\text{Li} + {}^{208}\text{Pb}$ (right) [19].

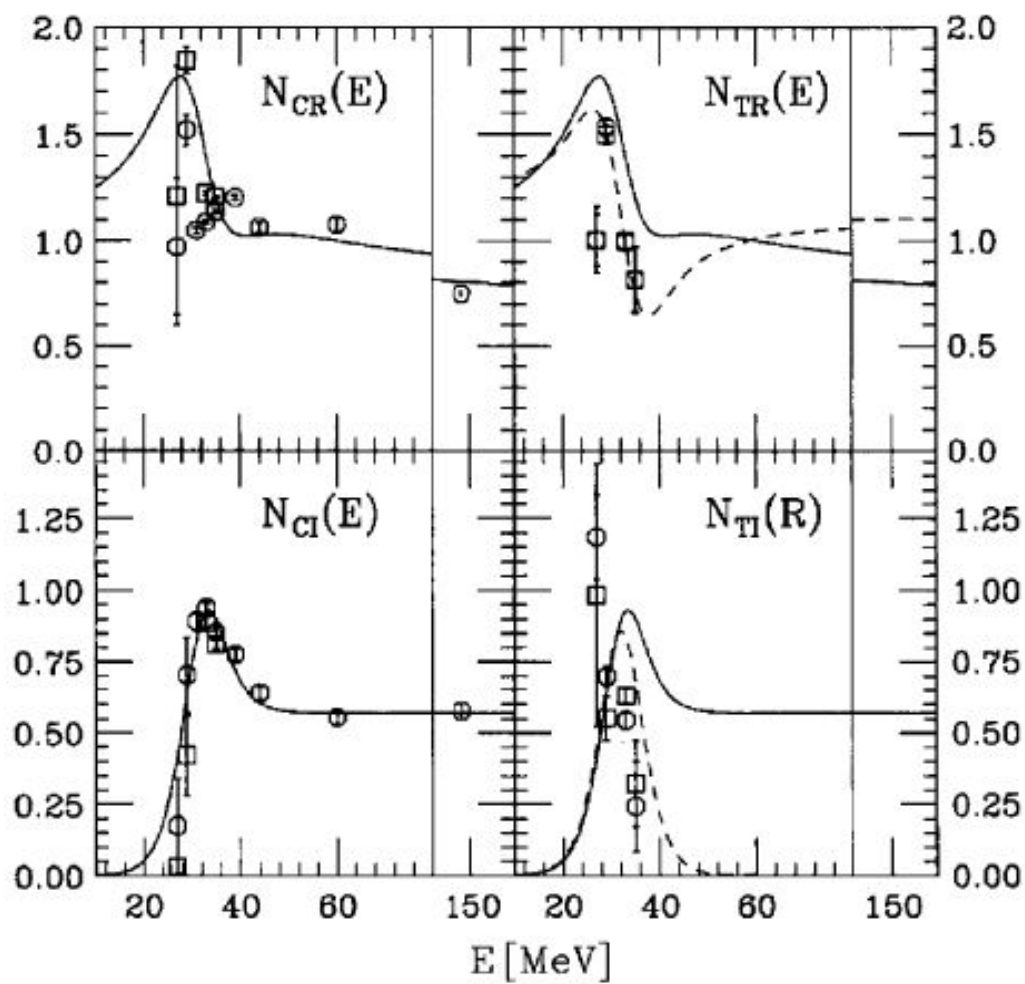


Figure 1.7 Best-fit real and imaginary central (left) and transition (right) terms of the nuclear potential, at the strong absorption radius, for the elastic scattering of polarized ${}^7\text{Li}$ on ${}^{208}\text{Pb}$ [24].

Maciel et al. [25] measured the elastic scattering for the ${}^6,7\text{Li} + {}^{138}\text{Ba}$ systems, at near barrier energies. The experimental angular distributions were analyzed through optical potentials of Woods–Saxon (WS) shape for the real and volume imaginary parts and a derivative WS form for the surface imaginary potential. The best-fit real and imaginary potentials, at the strong absorption radius, are shown in Figs. 1.8 and 1.9, for the ${}^6\text{Li} + {}^{138}\text{Ba}$ and ${}^7\text{Li} + {}^{138}\text{Ba}$ systems, respectively. The solid lines are results of the calculations using the dispersion relation for the optical potential. The dashed lines in Fig. 1.9 are results from CC calculations performed by Lubian et al. [26] when the ${}^7\text{Li}$ bound excited state is considered. One can see that the results are similar to those obtained for the ${}^{208}\text{Pb}$ target, although for the ${}^7\text{Li}$ just the coupling of the inelastic state of ${}^7\text{Li}$ is enough to destroy the threshold anomaly, contrary to the predictions by Keeley [19,20] concerning the importance of transfer channels.

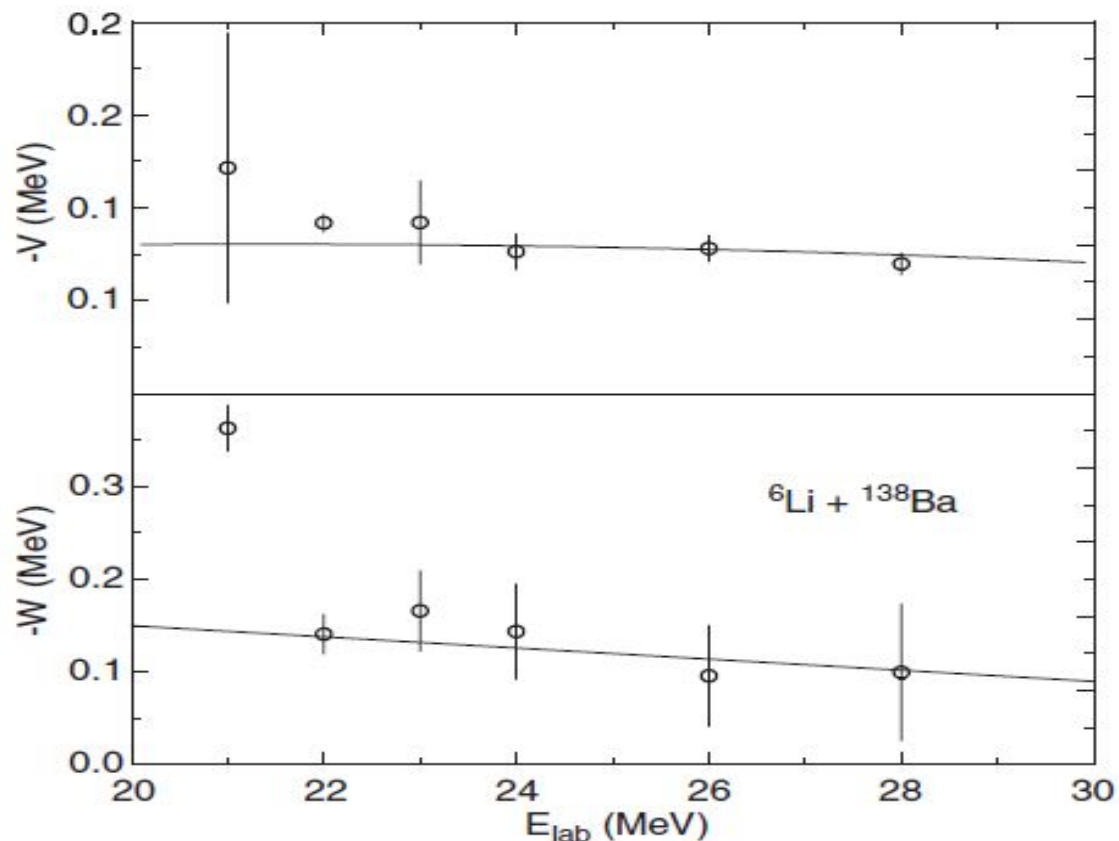


Figure 1.8 Best-fit real and imaginary potentials, at the strong absorption radius, for the elastic scattering of ${}^6\text{Li} + {}^{138}\text{Ba}$. The solid lines are calculations using the dispersion relation for the optical potential [25].

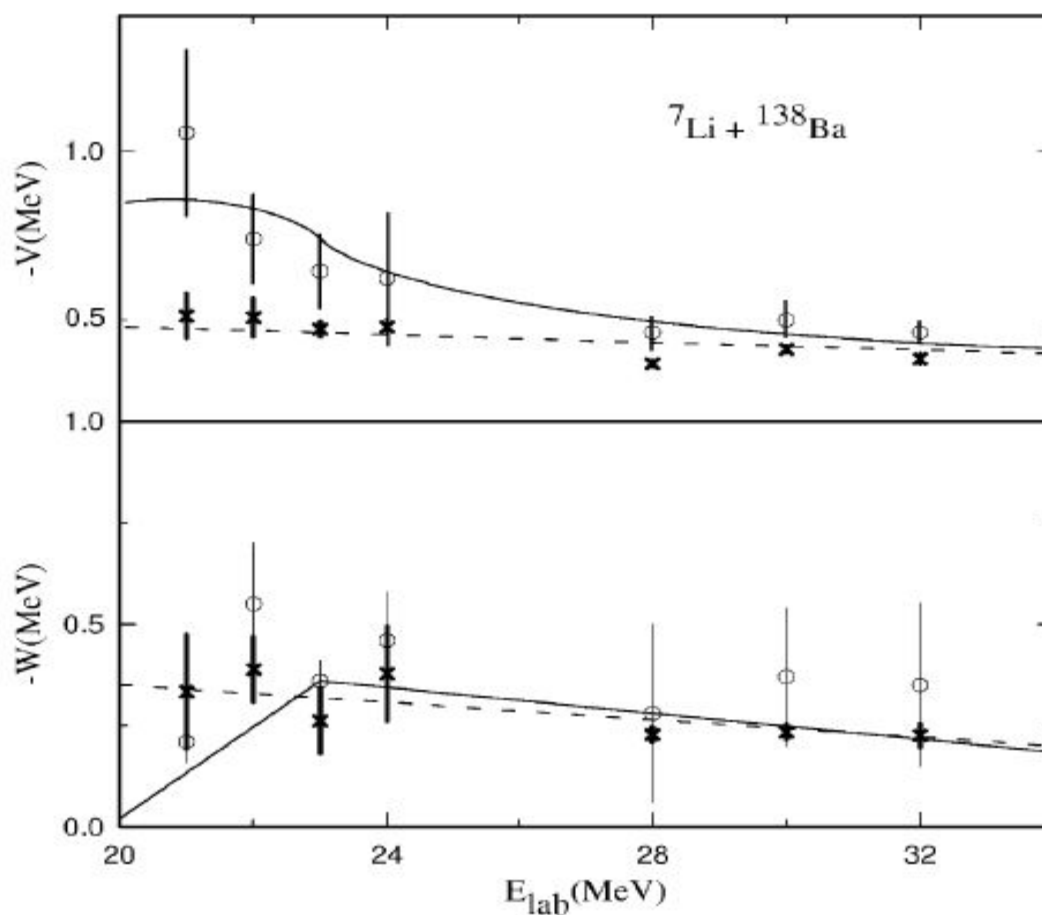


Figure 1.9 Best-fit real and imaginary potentials, at the strong absorption radius, for the elastic scattering of ${}^7\text{Li} + {}^{138}\text{Ba}$. The open points correspond to optical model calculations and the solid lines are results using the dispersion relation for the optical potential. The crosses correspond to CC calculations including the ${}^7\text{Li}$ first excited state, and the dashed curves are results using the dispersion relation and CC calculations [26].

The large values of the strength of the imaginary potential for ${}^6\text{Li}$, when compared with the ${}^7\text{Li}$ scattering on the same target, show that quasi-elastic reactions induced by ${}^6\text{Li}$ should dominate the reaction mechanisms at low energies, and the breakup process seems to be the main cause for the large reaction cross sections at near and sub-barrier energies. Actually, the reaction cross section for the ${}^6\text{Li} + {}^{138}\text{Ba}$ system is larger, at near barrier energies, than for ${}^7\text{Li} + {}^{138}\text{Ba}$, as can be seen in Fig. 1.10 [25].

The ${}^{6,7}\text{Li} + {}^{138}\text{Ba}$ elastic scattering data were re-analyzed by Hussein, Chamon and Gomes [27,28] using the São Paulo optical potential. Two parameters were used to fit the data, the normalization factors of the real and imaginary potentials, $N_R(E)$ and $N_I(E)$, respectively. The energy dependence of these normalizations takes into account the effects of the dynamic polarization potentials arising from direct channel couplings. The results are shown in Figs. 1.11 and 1.12, for ${}^6\text{Li}$ and ${}^7\text{Li}$, respectively. In both cases one can identify a new kind of Threshold Anomaly. This behavior, called Breakup Threshold Anomaly (BTA) [28,29], differs from the usual Threshold Anomaly (TA). So, this analysis confirms the results obtained by Maciel et al. [25] for the ${}^6\text{Li} + {}^{138}\text{Ba}$ system, but leads to different conclusions for the ${}^7\text{Li} + {}^{138}\text{Ba}$ system. More experimental data are required, at lower energies, in order to disentangle the behavior of ${}^7\text{Li}$ scattering, since a careful inspection of Fig. 1.7 may lead to the interpretation that the BTA might be present also for the ${}^7\text{Li} + {}^{208}\text{Pb}$ system. For the ${}^6\text{Li}$ scattering, it seems to be sure the presence of the BTA, as one can see also from Figs. 1.6–1.8.

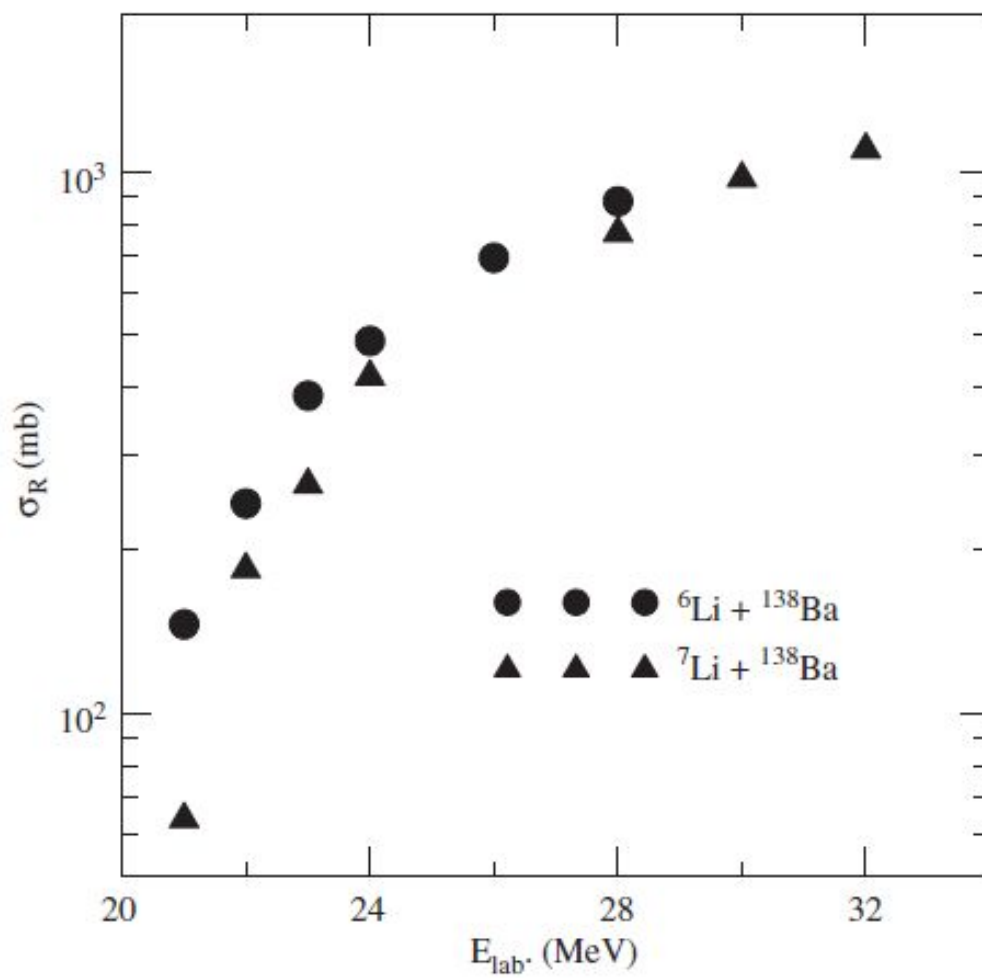


Figure 1.10 Reaction cross sections for the ${}^{6,7}\text{Li} + {}^{138}\text{Ba}$ systems [25].

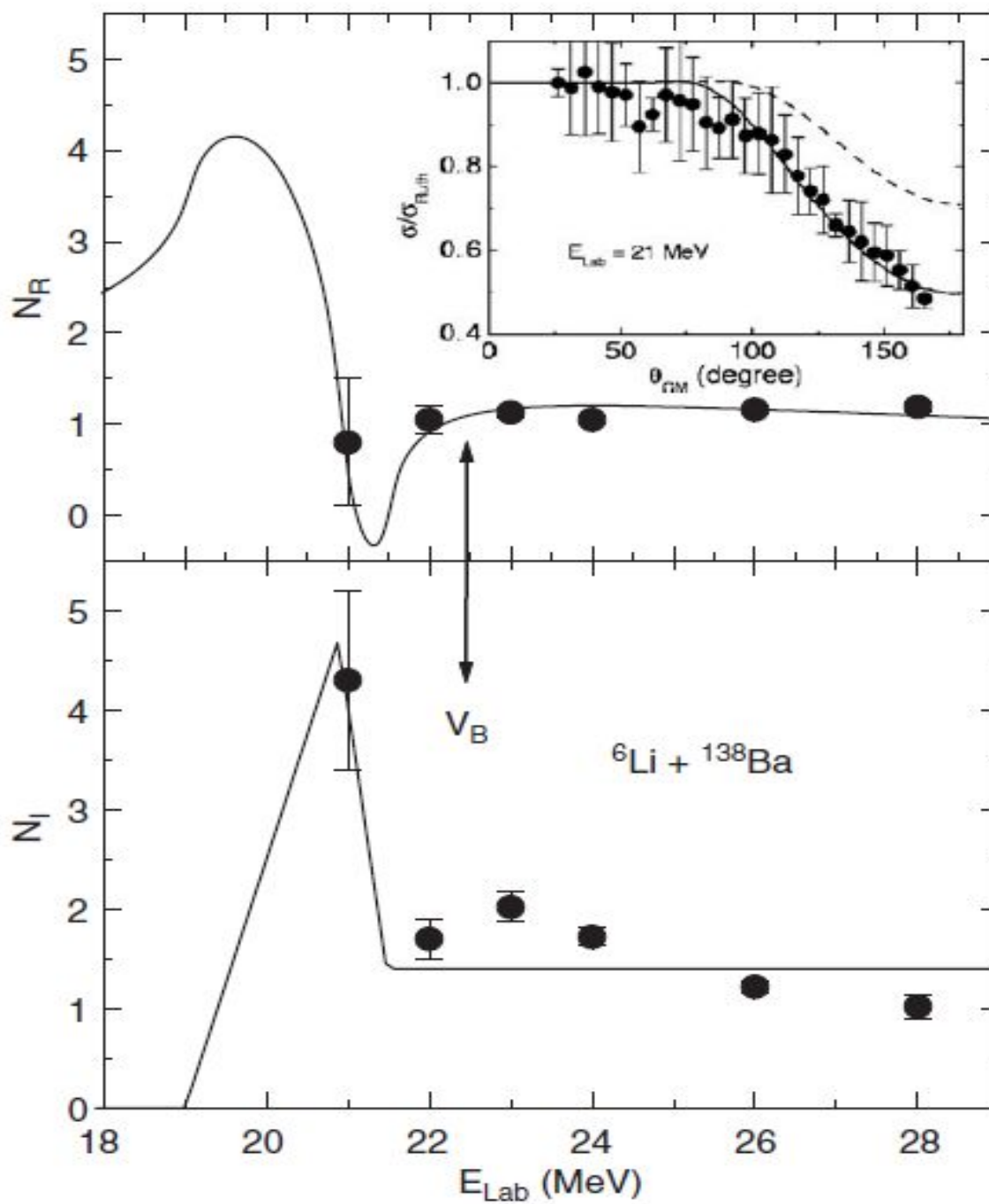


Figure 1.11 Energy dependence of the normalization factors N_R and N_I of the São Paulo potential which best fit the data, for the elastic scattering of ${}^6\text{Li} + {}^{138}\text{Ba}$. The solid lines are compatible with the dispersion relation [27,28].

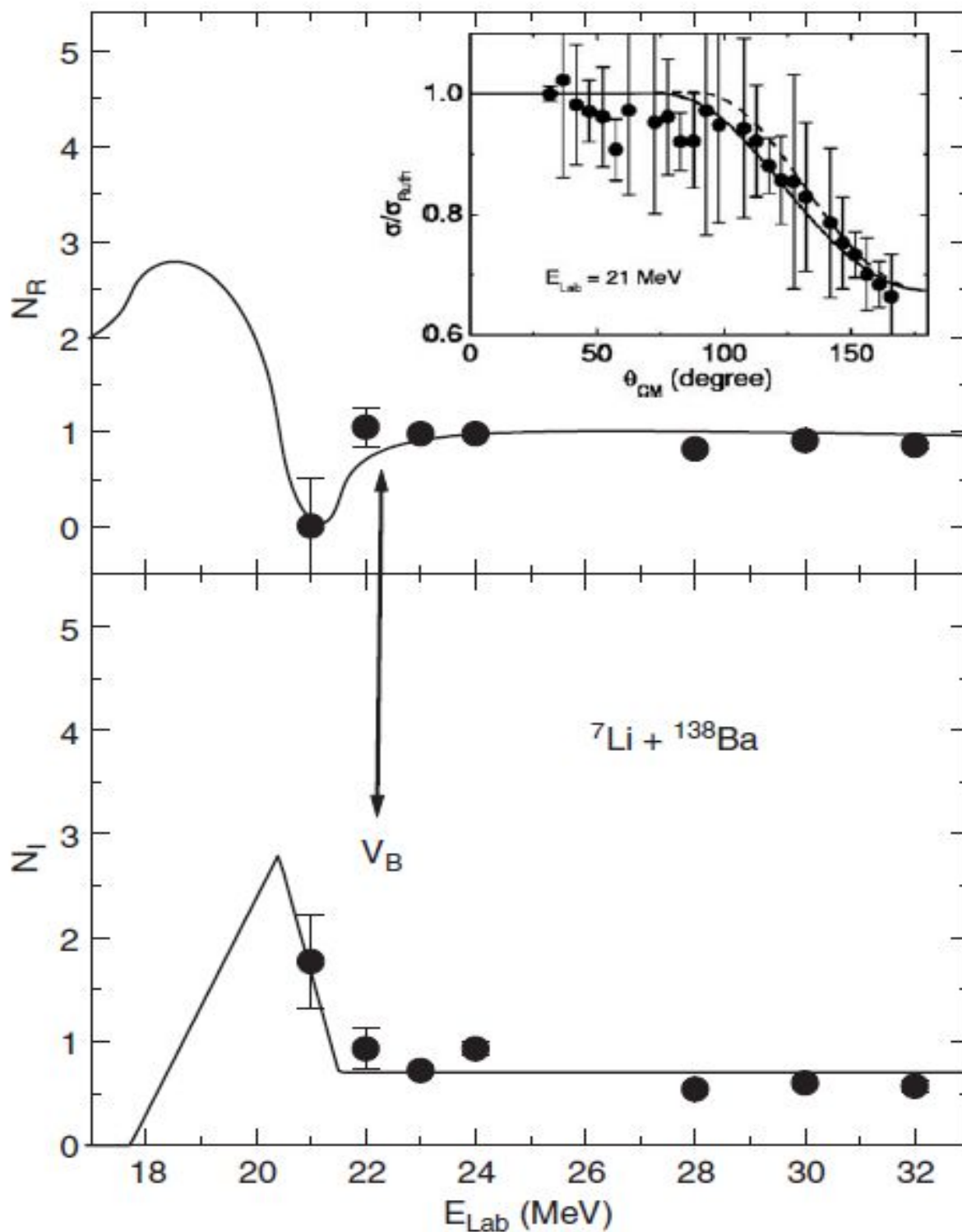


Figure 1.12 Energy dependence of the normalization factors N_R and N_I of the São Paulo potential which best fit the data, for the elastic scattering of ${}^7\text{Li} + {}^{138}\text{Ba}$. The solid lines are compatible with the dispersion relation [27,28].

The elastic scattering and transfer/breakup for the ${}^8\text{Li} + {}^{208}\text{Pb}$ system was measured by Kolata et al. [30], at energies around the Coulomb barrier. The ${}^8\text{Li}$ has threshold energy between those of ${}^6\text{Li}$ and ${}^7\text{Li}$, but its breakup leads to ${}^7\text{Li}$ and one neutron, instead of two charged fragments. The low beam intensity, and the consequently large error bars, did not allow any conclusion about the threshold anomaly. But, they lead to reaction cross sections which turned out to be much larger than those for ${}^7\text{Li}$. However, recently Gomez Camacho and Aguilera [31] performed direct reaction theory calculations on those data [30], in which a WS optical model is used. Fusion and direct parts of the imaginary potential are calculated separately, where the latter fits the one-neutron/breakup data, and the former fits the fusion cross sections derived from the difference between reaction and transfer/breakup cross sections. The direct part is the dominant imaginary potential and shows a behavior typical of the presence of the BTA, that is, there is a strong increase for decreasing energies around the barrier, whereas the fusion imaginary potential decreases slightly, that is a behavior typical of the usual threshold anomaly. The total optical potential for the ${}^8\text{Li}$ scattering, where the real part is calculated from dispersion relation, is found to show a similar behavior to the one for ${}^6\text{Li}$, that is, it is observed the presence of the BTA, caused in the present situation by the strong one-neutron/breakup channels at sub-barrier energies.

Significance of weakly bound, halo nuclei and radioactive ion beam

The study of light systems with very weakly bound and neutron rich exotic nuclei is particularly interesting, since there are reactions of great astrophysical interest involving these nuclei. As an example, in the case of inhomogeneous distribution of protons and neutrons following the Big Bang not only stable light elements but also proton and neutron rich short lived elements such as ${}^6\text{He}$, ${}^7\text{Be}$, ${}^8\text{B}$ and ${}^8\text{Li}$ would be present in the early universe. These, short lived, radioactive nuclei could thus bridge the $A=8$ mass gap and heavier elements would then be synthesized. Reactions involving light unstable nuclei would be present also in the type-II supernovae, neutron stars and in massive stars. Besides the triple alpha capture, the alpha recombination and the bridge of mass 5 and 8 in the beginning of the r-process in a type-II supernovae could be given via alternate three body reactions or sequential capture reactions such as ${}^4\text{He}(2n,\gamma){}^6\text{He}(2n,\gamma){}^8\text{He}$ [32]. In this case, the two neutron capture reaction cross sections on

^4He and ^6He depend strongly on the pronounced halo structure of the ^6He and ^8He compound nuclei.

1.5 Brief Literature Survey

In the past years, a lot of work has been performed to study reaction mechanisms in collisions induced by light, unstable (radioactive ion beams), halo, stable and weakly bound nuclei at energies around the Coulomb barrier. In particular, the effects of the breakup channel on the fusion and elastic scattering of weakly bound projectiles have been studied extensively, both experimentally and theoretically (Ref. [8] and references therein).

Especially much of the work has been carried out using the weakly bound nuclei $^{6,7}\text{Li}$ to study the threshold anomaly [16 – 18] in its elastic scattering. For these projectiles the breakup channel is expected to be important even at energies below the Coulomb barrier. The coupling to the breakup produces a repulsive polarization potential [33] and the usual TA may disappear. It has recently been suggested that a new kind of anomaly, known as the breakup threshold anomaly (BTA) [28,29], may be present in the scattering of weakly bound nuclei, where it has been observed that the strength of the imaginary potential even increases as the incident energy decreases. The cross-section of elastic scattering can help to obtain an optical potential which is necessary to understand the entrance and exit channel potentials of some transfer reactions. Breakup effects also play an important role in the scattering mechanism, affecting the interaction potential. One of the important points of investigation is whether the effect of breakup is essentially to increase the total reaction cross-section. Therefore, it is important to investigate the dependence of the breakup and total reaction cross-sections on the breakup threshold for different projectiles on light- and medium-mass targets.

The elastic scattering of the $^{6,7}\text{Li}$ projectiles around the Coulomb barrier energies has been studied with the variety range of targets, where for the system $^{6,7}\text{Li} + ^{208}\text{Pb}$ [29,34], $^{6,7}\text{Li} + ^{138}\text{Ba}$ [25], $^{6,7}\text{Li} + ^{59}\text{Co}$ [35], $^{6,7}\text{Li} + ^{28}\text{Si}$ [36,37], $^{6,7}\text{Li} + ^{27}\text{Al}$ [38,39], $^6\text{Li} + ^{58,64}\text{Ni}$ [40], $^6\text{Li} + ^{64}\text{Zn}$ [41], $^6\text{Li} + ^{90}\text{Zr}$ [42], $^{6,7}\text{Li} + ^{144}\text{Sm}$ [43], $^6\text{Li} + ^{209}\text{Bi}$ [44] suggests the absence of TA or it can be said that there is no conventional TA observed in the above cases. Thus the above systems are consistent with the presence of BTA. Thus our study also resembles the same, the investigation of BTA.

Moreover we also examined total reaction cross sections for a variety of systems consisting on weakly, tightly bound (stable) and radioactive proton or neutron halo projectiles on light targets. As has been shown in previous works [45–48] the total reaction cross-sections for the proton halo ${}^8\text{B}$ and borromean nucleus ${}^6\text{He}$ are larger than for no-halo projectiles.

1.6 Plan of the thesis

In the present thesis, effort has been made to measured precise elastic scattering angular distributions, at near barrier energies, for the weakly bound systems and two different energies for radioactive ion beams. The nuclei used, have very low breakup threshold energies and so they have a large breakup (BU) probability. At energies above the barrier, fusion cross sections are usually larger than BU cross sections, but at energies close to the barrier, the opposite occurs, and, furthermore, BU probabilities remain large even at energies below the Coulomb barrier. Thus using the weakly bound projectiles a system is said to follow the phenomenon called breakup threshold anomaly (BTA). The analysis to check the energy dependence of the interacting potentials of the optical potentials were performed using the phenomenological Woods-Saxon form interaction potential and double-folding Sao Paulo potential (SPP). In continuation we have also compared the total reaction cross sections for several systems to provide the theoretical background for our conclusions. The target ${}^{116,112}\text{Sn}$ was used for the weakly bound projectiles with significance to fill the gap between $A = 59$ and 144 for the target mass. In the case of radioactive ion beam the corresponding total reaction cross-sections were available in the literature for one energy ($E_{\text{lab}} = 26$ MeV) for the ${}^8\text{Li} + {}^{51}\text{V}$ system [49] and two energies (14 MeV and 27 MeV) [50,51] for the ${}^8\text{Li} + {}^9\text{Be}$ system. Thus the new measurement of elastic scattering cross-section for ${}^8\text{Li} + {}^9\text{Be}$ and ${}^8\text{Li} + {}^{51}\text{V}$ systems were done at 19.6 MeV and 18.5 MeV, respectively. Analyses were performed for previously reported data for these systems and for many other light systems. Here also the total reaction cross sections were extracted and comparison with several systems was carried out.

The thesis is planned into six chapters, as discussed below.

In **Chapter 1**, general introduction is given regarding the nuclear reactions, brief review of the nuclear physics far from the stability line, that is, the current interest and development in

the study of unstable nuclei. Also in a concise manner some introduction to the heavy ion induced nuclear reactions being shown. Then we have discussed the necessity to study the reactions involving weakly bound, halo nuclei and radioactive ion beam over the tightly bound nuclei. At the completion of this chapter we briefly mentioned regarding the literature survey and the motivation of the thesis.

In **Chapter 2**, brief descriptions of the model used have been given, and how the model which we have used is of prime importance for our study has been shown. To check the consistency of the results obtained, we analyzed our data using two different kinds of potential so as to observe the model's independency. So regarding those two different kinds of the potential has also been mentioned in this chapter.

In **Chapter 3**, we discuss about the measured elastic scattering of the weakly bound ${}^6\text{Li}$ on the ${}^{116,112}\text{Sn}$ targets, at energies close to the Coulomb barrier [52]. Here we will discuss the experimental procedure used for detecting the elastically scattered particles, detectors used and their basic working principles, data analysis and the theoretical calculations using the Optical model and the code used. Also we will show the extraction of the total reaction cross sections of our system and comparison of it with various systems. At the end we will discuss the elucidation of our derived results and conclusions.

In **Chapter 4**, our extension of the work will be presented with replacement of the projectile of ${}^6\text{Li}$ with ${}^7\text{Li}$ on ${}^{116}\text{Sn}$ target. Here also briefly the experimental procedure and etc., will be discussed along with extraction of the total reaction cross sections of ${}^7\text{Li} + {}^{116}\text{Sn}$ system and comparison of it with previous ${}^6\text{Li} + {}^{116}\text{Sn}$ system [53,54] and other systems [55]. At the end we will discuss the elucidation of our derived results and conclusions.

In **Chapter 5**, we will be discussing the experiment carried out at the Brazil using the radioactive ion beam facility therein. We have obtained the beam of ${}^8\text{Li}$ that was bombarded on the two different targets ${}^9\text{Be}$ and ${}^{51}\text{V}$ and similarly the elastic scattering angular distribution were measured but here the energies covered was less in number, as the beam produced was the secondary beam and the intensity was lower, so more sets of energy were difficult to cover. So here also how the radioactive ion beam produced, facility developed, detectors used etc., is discussed along with the data analysis and the theoretical calculations using the Optical model. Again the extraction of the total reaction cross sections for the mentioned system and comparison

of it with several systems has been shown [56]. At the end we will discuss the elucidation of our derived results and conclusions.

In **Chapter 6**, we will present the summary and conclusions of our present effort along with the future outlook.

References

- [1] I. Tanihata *et al*, Phys. Lett. **B160**, 380 (1985).
- [2] I. Tanihata *et al*, Phys. Rev. Lett. **55**, 2676 (1985).
- [3] H. Feshbach, Theoretical Nuclear Physics, Vol.1, Wiley, New York (1992).
- [4] K.S. Krane, Introductory Nuclear Physics, Wiley, Canada 242 (1988).
- [5] N.K. Glendenning., Rev. Mod. Phys. **47**, 659 (1975).
- [6] W.U. Schroder and J.R. Huizenga, Treatise on Heavy-ion Science, Vol.2 ed. D.A. Bromley (Plenum), New York, London, (1984).
- [7] K.H. Schmidt and W. Morawek, Rep. Prog. Phys. **54**, 949 (1991).
- [8] L.F. Canto, P.R.S. Gomes, R. Donangelo, M.S. Hussein, Phys. Rep. **424**, 1 (2006).
- [9] R.Raabe *et al*, Nature **431**, 823 (2004).
- [10] M. Kawai, Prog. Theor. Phys. (Suppl.) **89**, 11(1986).
- [11] N. Austern *et al*, Phys. Rep. **154**, 125 (1987).
- [12] A. Diaz-Torres, I.J. Thompson, Phys. Rev. C **65**, 024606 (2002).
- [13] L.F. Canto, R. Donangelo, L.M. de Matos, M.S. Hussein, P. Lotti, Phys. Rev. C **58**, 1107 (1998).
- [14] M.S. Hussein, K.W. McVoy, Nucl. Phys. A **445**, 124 (1985).
- [15] M.S. Hussein, B.V. Carlson, T. Frederico, T. Tarutina, Nucl. Phys. A **738**, 367 (2004).
- [16] M.A. Nagarajan, C.C. Mahaux, G.R. Satchler, Phys. Rev. Lett. **54**, 1136 (1985).
- [17] G.R. Satchler, Phys. Rep. **199**, 147 (1991).
- [18] M.E. Brandan, G.R. Satchler, Phys. Rep. **285**, 143 (1997).
- [19] N. Keeley *et al.*, Nucl. Phys. A **571**, 326 (1994).
- [20] N. Keeley, K. Rusek, Phys. Rev. C **56**, 3421 (1997).
- [21] N. Keeley, K. Rusek, Phys. Lett. B **427**, 1 (1998).
- [22] N. Keeley, K.W. Kemper, K. Rusek, Phys. Rev. C **66**, 044605 (2002).
- [23] I. Martel *et al.*, Nucl. Phys. A **582**, 357 (1995).
- [24] I. Martel *et al.*, Nucl. Phys. A **605**, 417 (1996).
- [25] A.M.M. Maciel *et al.*, Phys. Rev. C **59**, 2103 (1999).
- [26] J. Lubian *et al.*, Phys. Rev. C **64**, 027601 (2001).

- [27] M.S. Hussein, L.C. Chamon, P.R.S. Gomes, in: Proceedings of the Workshop on Reaction Mechanisms of Rare Isotopes, MSU, USA, 2005, AIP Conf. Ser. **791**, 140 (2005).
- [28] P.R.S. Gomes *et al.*, J. Phys. G **31**, S1669 (2005).
- [29] M. S. Hussein, P. R. S. Gomes, J. Lubian, and L. C. Chamon, Phys. Rev. C **73**, 044610 (2006).
- [30] J.J. Kolata *et al.*, Phys. Rev. C **65**, 054616 (2002).
- [31] A. Gomez Camacho, E.F. Aguilera, Nucl. Phys. A **735**, 425 (2004).
- [32] J. Gorres, *et al.*, Phys. Rev. C **52**, 2231 (1995).
- [33] Y. Sakuragi, Phys. Rev. C **35**, 2161 (1987).
- [34] M. S. Hussein, P. R. S. Gomes, J. Lubian, and L. C. Chamon, Phys. Rev. C **76**, 019902(E) (2007).
- [35] F. A. Souza *et al.*, Phys. Rev. C **75**, 044601 (2007).
- [36] A. Pakou *et al.*, Phys. Lett. B **556**, 21 (2003).
- [37] A. Pakou *et al.*, Phys. Rev. C **69**, 054602 (2004).
- [38] J.M. Figueira *et al.*, Phys. Rev. C **75**, 017602 (2007).
- [39] J.M. Figueira *et al.*, Phys. Rev. C **73**, 054603 (2006).
- [40] M. Biswas *et al.*, Nucl. Phys. A **802**, 67 (2008).
- [41] M. Zadro *et al.*, Phys. Rev. C **80**, 064610 (2009).
- [42] H. Kumawat *et al.*, Phys. Rec. C **78**, 044617 (2008).
- [43] J.M. Figueira *et al.*, Phys. Rev. C **81**, 024613 (2010).
- [44] S. Santra *et al.*, Phys. Rev. C **83**, 034616 (2011).
- [45] J.M.B. Shorto *et al.*, Phys. Lett. B **678**, 77 (2009).
- [46] J.J. Kolata, E.F. Aguilera, Phys. Rev. C **79**, 027603 (2009).
- [47] E.F. Aguilera *et al.*, Phys. Rev. C **80**, 044605 (2009).
- [48] A. Barioni *et al.*, Phys. Rev. C **84**, 014603 (2011).
- [49] R. Lichtenthäler *et al.*, AIP Conf. Proc. **1139**, 76 (2009).
- [50] O. Camargo *et al.*, Phys. Rev. C **78**, 034605 (2008).
- [51] F.D.Becchetti *et al.*, Phys. Rev. C **48**, 308 (1993).
- [52] N. N. Deshmukh *et al.*, Phys. Rev. C **83**, 024607 (2011).

- [53] N.N. Deshmukh *et al.*, Eur. Phys. J A **47**, 118 (2011).
- [54] N.N. Deshmukh *et al.*, AIP Conference Proceedings, **1423**, 122 – 125 (2012) (IX – Latin America Symposium on Nuclear Physics and Applications, 2011).
- [55] N.N. Deshmukh *et al.*, Proceedings of National Conference on Emerging Interfaces of Physics and Technology – 2011 (EIPT – 2011), Excel India Publishers (ISBN: 978-93-81361-31-3), Page 108 – 111.
- [56] S. Mukherjee, N. N. Deshmukh *et al.*, Eur. Phys. J. A **45**, 23 – 28 (2010).